

Langevin Evolution of Disoriented Chiral Condensate

Luís M. A. Bettencourt^{1,2}, Krishna Rajagopal¹ and James V. Steele¹

¹ *Center for Theoretical Physics, Massachusetts Institute of Technology, Cambridge MA 02139*

² *Theoretical Division, MS B288, Los Alamos National Laboratory, Los Alamos NM 87545*

(November 6, 2018)

Abstract

As the matter produced in a relativistic heavy ion collision cools through the QCD phase transition, the dynamical evolution of the chiral condensate will be driven out of thermal equilibrium. As a prelude to analyzing this evolution, and in particular as a prelude to learning how rapid the cooling must be in order for significant deviations from equilibrium to develop, we present a detailed analysis of the time-evolution of an idealized region of disoriented chiral condensate. We set up a Langevin field equation which can describe the evolution of these (or more realistic) linear sigma model configurations in contact with a heat bath representing the presence of other shorter wavelength degrees of freedom. We first analyze the model in equilibrium, paying particular attention to subtracting ultraviolet divergent classical terms and replacing them by their finite quantum counterparts. We use known results from lattice gauge theory and chiral perturbation theory to fix nonuniversal constants. The result is a theory which is ultraviolet cutoff independent and that reproduces quantitatively the expected equilibrium behavior of the quantum field theory of pions and σ fields over a wide range of temperatures. Finally, we estimate the viscosity $\eta(T)$, which controls the dynamical timescale in the Langevin equation, by requiring that the timescale for DCC decay agrees with previous calculations. The resulting $\eta(T)$ is larger than that found perturbatively. We also determine the temperature below which the classical field Langevin equation ceases to be a good model for the quantum field dynamics.

PACS: 11.10.Wx, 12.38.Mh, 11.30.Rd, 25.75.-q

arXiv:hep-ph/0106257v2 18 Jul 2001

I. INTRODUCTION

The relativistic heavy-ion collider (RHIC) is now creating strongly-interacting matter at high enough energy density that there is every expectation that temperatures above the QCD phase transition are being explored. The question of equilibration is crucial to the understanding of these collisions. There has been much progress on one aspect of this question recently: we now know that (at least at arbitrarily high collision energies) an equilibrated quark-gluon plasma *will* be created [1]. Furthermore, the first analyses of elliptic flow data can be interpreted as indicating early thermalization in RHIC collisions [2]. What remains quite unclear, however, is whether even if an equilibrated partonic medium is attained early in the collision, thermal equilibrium is maintained as the matter cools through the QCD phase transition and becomes a gas of hadrons, which subsequently freeze out and are seen in a detector.

The QCD phase transition is likely a smooth crossover if it is traversed at low baryon number chemical potential μ_B . At larger μ_B , it is thought to be first order. This means that at a critical μ_B , there is a second order phase transition in the universality class of the three-dimensional Ising model [3–6]. The nature of the possible nonequilibrium phenomena are quite different in these three cases [7]. If the transition is first order, bubbling may yield a spatially inhomogeneous final state [8]. If the transition occurs near the second order critical point, then nonequilibrium effects tend to obscure the unique fluctuations characteristic of the equilibrium critical point: in equilibrium, the correlation length would diverge there; nonequilibrium effects smooth out this divergence [9]. The farther from equilibrium the evolution is, the less likely are distinctive signatures of the critical point. Finally, if the transition is a crossover, as is likely at RHIC where μ_B is small, and if this crossover is traversed sufficiently quickly that the dynamics can be treated as a “maximally out of equilibrium” quench, then long wavelength oscillations of the chiral condensate are excited to amplitudes which are greatly in excess of those present in equilibrium [10]. The primary signal of these disorientations of the chiral condensate (DCC) is a large number of soft pions exhibiting large fluctuations in isospin [11–14,10], which have been looked for and not seen in lower energy heavy ion collisions at the CERN SPS [15]. Many other DCC signatures have also been discussed [16]. The crucial unresolved question in all three cases is: “How rapid must the cooling be in order for the evolution to deviate significantly from thermal equilibrium?” In this paper, we lay the ground work for answering this question in the case of a smooth crossover.

We construct a Langevin description of the nonequilibrium dynamics of the chiral condensate which we can use over a range of temperatures around the phase transition. Our dynamical degrees of freedom are those of the classical linear sigma model. This is valid as long as m_σ and m_π are much smaller than the temperature. It is therefore valid near T_c sufficiently close to the chiral limit. We shall use it with parameters chosen to reproduce the physical pion mass at zero temperature, and this will mean that we are using the classical theory beyond its realm of quantitative validity. Until quantum field theoretical approaches (for example those of Refs. [17]) mature to the point where they can be used to describe spatially varying field configurations, the present classical analysis is of value as a guide.

Why introduce a Langevin heat bath? That is, why go beyond the purely classical analysis of Refs. [10,18]? Allowing the long wavelength degrees of freedom to exchange

energy with a heat bath is a crude way of representing the existence of other degrees of freedom. Our reason for introducing it is that we wish to investigate the response of the long wavelength degrees of freedom to decreases in the temperature T of the heat bath that occur with varying speeds. If T is reduced arbitrarily slowly, the system must stay arbitrarily close to equilibrium. If T is reduced suddenly, nonequilibrium dynamics results. With a Langevin equation, therefore, we shall be able to learn how fast the cooling must be in a heavy ion collision if the traversal of the crossover region of the phase transition is to be associated with DCC phenomena. In addition to a time varying heat bath temperature, we shall also be able to use the freedom to let T vary as a function of position to consider initial conditions in which the hot region is finite in extent.

We leave the answer to the questions just posed to a subsequent paper. Here, we focus on setting up the Langevin description, and choosing all the associated parameters. Many parameters can be chosen entirely with reference to properties of the system in thermal equilibrium. We can fix these parameters by comparison with known results from chiral perturbation theory and lattice gauge theory. In so doing we obtain a Langevin equation which gives a reasonable description of the equilibrium physics from very low temperatures up to temperatures well above T_c . This is possible in equilibrium, but the classical description of *dynamics* must break down at low temperatures, where $m_{\sigma,\pi} \gg T$. We discover this breakdown when we seek to fix those parameters in the Langevin equation which require dynamical input, namely the viscosity $\eta(T)$. To this end, we analyze the decay of an idealized DCC with time, due to the presence of the heat bath. This problem has been analyzed previously by Steele and Koch [19], and we use their results to fix the viscosity in our Langevin equation. We find that in the vicinity of T_c , where we expect our treatment to be valid, we can successfully reproduce the DCC decay timescale of Ref. [19]. In order to do so, the η we introduce is about a factor of five larger than that predicted by perturbative calculation [20]. At lower temperatures, the whole analysis breaks down: even with the dissipation due to the heat bath completely removed by setting η to zero, we find that the DCC decays much more quickly than it should. The long wavelength DCC is decaying not via interaction with the stochastic heat bath but via its interactions with modes which we are treating classically. We are therefore able to evaluate the temperature below which our classical Langevin field equation should not be used to model the dynamics.

Our analysis complements that in several previous papers. Greiner and Müller [21] and Rischke [20] have derived effective Langevin equations by integrating out hard modes perturbatively and found that these typically include correlated and multiplicative sources of noise and dissipation. Xu and Greiner [22] then explored the effects of such noise and dissipation on $0 + 1$ -dimensional dynamics. This treatment of the noise goes beyond ours, since we treat the heat bath as an uncorrelated source of fluctuation. However, whereas $0 + 1$ -dimensional calculations (like those of Refs. [22,23]) treat the dynamics of only one mode explicitly and thus assume spatial homogeneity, our $3 + 1$ -dimensional Langevin equation allows an analysis of more realistic, spatially varying, configurations. The $3 + 1$ -dimensional Langevin equation has been introduced previously by Chaudhuri [24], although as he notes in Ref. [25] all of his results depend sensitively on his choice of lattice spacing. We introduce the correct T -dependent counterterms in order to obtain results at long wavelengths which are independent of the lattice-spacing. Randrup has addressed the linear sigma model dynamics in a series of papers, using either the classical theory or a Hartree approximation [26].

These studies have shown the importance of accounting correctly for the multidimensional expansion of the hot system, and have provided initial answers to some of the questions we wish to investigate. The stochastic linear sigma model we develop below has the relative advantage of having dynamics which equilibrate at late times in the absence of expansion and in addition allows us to take some account of the effects of shorter wavelength degrees of freedom on the longer wavelength modes we treat classically.

In Section II we describe the model, paying close attention to the counterterms which are needed in order to ensure that the long wavelength physics is not divergent as the lattice spacing is taken to zero. In Section III, we evaluate the order parameter as a function of temperature and fix the most important finite counterterms by enforcing agreement with chiral perturbation theory at low temperature and with lattice gauge theory calculations of the critical temperature. We also evaluate the temperature-dependent pion and sigma masses. In Section IV, we analyze the decay of a DCC. By comparing the DCC lifetime we obtain to that calculated previously by other methods, we fix the viscosity η in the Langevin equation, which couples the classical fields to the heat bath. We also determine the temperature below which a classical field treatment fails to describe the dynamics correctly. We close in Section V with a look towards the future.

II. LANGEVIN EQUATIONS AND COUNTERTERMS

At low temperatures, the correct effective field theory for QCD is the nonlinear sigma model, describing the dynamics of the pseudoscalar pions. At the QCD phase transition, however, chiral symmetry is approximately restored and the scalar sigma becomes approximately degenerate with the pions. These four degrees of freedom are the lightest in QCD near its finite temperature phase transition. Indeed, if the up and down quarks were massless, these four modes would all be massless at T_c , making the transition an $O(4)$ second order phase transition [27,14]. Lattice QCD calculations suggest that with quark masses as in nature, these modes have inverse correlation lengths which are comparable to T_c [28]. This means that although these modes are still the lightest degrees of freedom, the classical treatment we employ is at or beyond the limit of its regime of validity. Two asides should be noted at this point. First, at the μ_B at which there is a second order critical point in the QCD phase transition, the sigma becomes massless while the pions do not. Second, there have been recent suggestions that the lightest scalar glueball may play an interesting role at the transition [29]. Lattice QCD calculations show that this has a correlation length close to $(3T_c)^{-1}$ [30], much shorter than that of the pion [31], and we therefore neglect it.

Writing the pions and the sigma as an $O(4)$ vector $\phi_a = (\sigma, \vec{\pi})$, the linear sigma model Lagrangian is given by

$$\mathcal{L} = \frac{1}{2} \partial_\mu \phi_a \partial^\mu \phi_a - \frac{\lambda}{4} (\phi_a^2 - v^2)^2 + H\sigma, \quad (1)$$

with summation over repeated indices implied. The context in which this is of precise validity is two-flavor QCD in the chiral limit, on the assumption that this theory has a second order phase transition, as is consistent with what we know from lattice QCD calculations [32]. Then, that transition is in the same $O(4)$ universality class as the second order phase transition found at nonzero temperature in the theory (1) with $H = 0$ [27,14]. The explicit

symmetry breaking term H , the coupling λ , and the vacuum expectation value v can be expressed in terms of the phenomenological parameters m_σ , m_π , and f_π at tree level via

$$H = f_\pi m_\pi^2, \quad \lambda = \frac{m_\sigma^2 - m_\pi^2}{2f_\pi^2}, \quad v^2 = \frac{m_\sigma^2 - 3m_\pi^2}{m_\sigma^2 - m_\pi^2} f_\pi^2. \quad (2)$$

We take $(f_\pi, m_\pi, m_\sigma) = (92.4, 135, 600)$ MeV, meaning $H = (119. \text{ MeV})^3$, $\lambda = 20.0$ and $v = 87.3$ MeV.

The simplest Langevin prescription corresponds to including additive stochastic sources $\xi_a(x, t)$ and dissipation terms in the Euler-Lagrange equations of motion for the fields:

$$\frac{\partial^2 \phi_a}{\partial t^2} - \nabla^2 \phi_a + \lambda (\phi_a^2 - v^2) \phi_a - H \delta_{a0} = -\eta_{ab} \frac{\partial \phi_b}{\partial t} + \xi_a. \quad (3)$$

The stochastic fields ξ_a are taken to obey the fluctuation-dissipation relations

$$\langle \xi_a(x) \xi_b(y) \rangle = 2\eta_{ab}(x) T \delta^4(x - y), \quad (4)$$

with $\langle \xi_a(x) \rangle = 0$. In this paper, we shall always choose $\eta_{ab}(x) = \eta(T) \delta_{ab}$. This dynamics reduces to the classical microcanonical relativistic evolution for the pions and sigma in the limit of small dissipation $\eta \rightarrow 0$. In the limit of vanishing masses the long wavelength modes of the fields are effectively overdamped, and suffer critical slowing down [33]. Then our equations correspond to Model A, in the classification of dynamical stochastic theories of Hohenberg and Halperin [34]. Although Model A will be adequate for our purposes, a complete analysis of the universal $O(4)$ dynamics in the chiral limit of QCD requires coupling the order parameter (which is not conserved) to other conserved quantities in the theory, as in Hohenberg and Halperin's Model G [14].

For any nonzero value of η , at late times ($t \gg \eta^{-1}$) the Langevin dynamics describes evolution towards a steady state characterized by the equilibrium partition function

$$\mathcal{Z} = N \int D\phi E^{-\beta \mathcal{H}[\phi]}, \quad (5)$$

with

$$\mathcal{H}[\phi] = \int d^3x \left[\frac{1}{2} (\nabla \phi_a)^2 + \frac{\lambda}{4} (\phi_a^2 - v^2)^2 - H \sigma \right]. \quad (6)$$

Eq. (5) is the canonical partition function for the linear sigma model in 3D. Note that the ensemble of equilibrium configurations described by this partition function is independent of η . In this section and the next, we shall use equilibrium physics to fix all parameters in the model except η . In Section IV, we shall fix η by analyzing the dynamics of the relaxation of nonequilibrium configurations towards equilibrium.

Eq. (5) is the correct equilibrium state for the *classical* model. When compared to the quantum partition function it fails to account for the correct statistical weighting of hard particles (with typical momentum $k \sim T$) and at low temperatures, when ($T < m_\pi, m_\sigma$). We will return to the latter point in the next section. The classical statistical weighting of hard modes in the equilibrium state leads to ultraviolet divergences (as the lattice spacing a_s is taken to zero) of certain expectation values at nonzero temperature. This effect is an



FIG. 1. The two perturbative diagrams that are ultraviolet divergent in the classical theory at finite temperature: a) the tadpole and b) the sunset. Both divergences are momentum independent allowing us to compute the sunset diagram at zero external momentum only.

incorrect prediction of the classical partition function. Fortunately it can be compensated for. The idea is to subtract the divergent terms, which are all perturbative and can therefore be identified diagrammatically. These are then replaced by the corresponding correct contributions, identified through the computation of the same diagram using quantum statistical distributions.

For the linear sigma model in three dimensions, there are only two divergent diagrams, shown in Fig. 1. These are self-energy contributions: the tadpole diagram at one loop and the sunset diagram at two loops [35]. Both divergences are momentum independent and can be subtracted away by a simple temperature dependent mass renormalization. These two diagrams can be written as

$$I_{\text{tadpole}} = \frac{4!}{2!} \frac{\lambda}{4} \frac{N+2}{3} \int \frac{d^3k}{(2\pi)^3} G(\omega_k), \quad (7)$$

$$I_{\text{sunset}} = \frac{4!^2}{3!} \left(\frac{\lambda}{4}\right)^2 \frac{N+2}{3} \int \frac{d^3k d^3q}{(2\pi)^6} \frac{G(\omega_k)G(\omega_q)}{|\vec{k} + \vec{q}|^2 + m^2}. \quad (8)$$

We have made explicit all symmetry factors. The two-point function for the scalar field $G(\omega)$ has the thermal (no vacuum contributions) form $G(\omega) = n(\omega)/\omega$, with the single particle number distribution given by

$$n(\omega) = \begin{cases} \frac{T}{\omega}, & \text{classical,} \\ \frac{\hbar}{e^{\hbar\omega/T} - 1}, & \text{Bose-Einstein,} \end{cases} \quad (9)$$

for classical or quantum scalar fields respectively. Clearly, the quantum distribution approaches the classical for $\hbar\omega/T \rightarrow 0$, i.e., in the limit of high occupation numbers. Ultimately this is why the classical theory becomes a good description of long wavelength physics when masses are vanishing or at least small compared to T , as happens at a true critical point.

On the lattice, the continuum dispersion relation for a particle of mass m , namely $\omega^2 = k^2 + m^2$, becomes

$$\omega^2 = \frac{4}{a_s^2} \sum_{i=1}^D \sin^2\left(\frac{k_i a_s}{2}\right) + m^2, \quad (10)$$

where a_s is the lattice spacing and D the number of spatial dimensions. Here, $k_i = 2\pi n_i/N_i a_s$, with N_i the linear size of the lattice and $n_i \in \{-\frac{1}{2}N_i, \frac{1}{2}N_i\}$, for each Euclidean dimension. Eq. (10) reduces to the continuum result when $k_i a_s$ is small.

If we are interested only in the ultraviolet behavior of the tadpole diagram Fig. 1a, we can neglect the mass m . (This diagram has no infrared divergences.) This yields

$$I_{\text{tadpole}}^{\text{cl}} = \frac{N+2}{2\pi^2} \lambda T \Lambda \rightarrow 0.25 \frac{(N+2)\lambda T}{a_s}, \quad (11)$$

$$I_{\text{tadpole}}^{\text{B-E}} = \frac{N+2}{12} \frac{\lambda T^2}{\hbar}. \quad (12)$$

The classical tadpole is linearly divergent with the ultraviolet momentum cutoff Λ . The arrow shows the result on the lattice, from summing over modes within a Brillouin zone. To the accuracy quoted, these lattice results are identical for $N_i \geq 32$ and various temperatures. The Bose-Einstein tadpole is finite.

The sunset diagram Fig. 1b, has only a logarithmic divergence and so in addition to being ultraviolet divergent it is infrared divergent in the absence of masses [36]. Since only the difference of the two contributions $I^{\text{B-E}} - I^{\text{cl}} \equiv \Delta I$ enters our calculation, the infrared divergence cancels out (allowing us again to neglect the mass m) and the ultraviolet divergence is $(N+2)\lambda^2 T^2 \ln(T/\hbar\Lambda)/8\pi^2$. There is no convenient analytic form for the finite part, but on the lattice the result is

$$\Delta I_{\text{sunset}} \rightarrow [0.0144 \ln(Ta_s/\hbar) - 0.0369] (N+2)\lambda^2 T^2. \quad (13)$$

The renormalization is then achieved by making the replacement

$$-\lambda v^2 \rightarrow -\lambda v^2 + \Delta I_{\text{tadpole}} + \Delta I_{\text{sunset}} \quad (14)$$

in the term linear in ϕ_a in the equation of motion Eq. (3), which removes the linear and logarithmic divergences in the self energy. Note that $\Delta I \rightarrow 0$ as $T \rightarrow 0$, and so this renormalization does not affect the choice of the parameters in Eq. (2) at zero temperature. This is true to all loop orders. The procedure we have described implements the matching of the classical thermal theory to the quantum in the ultraviolet, where the classical partition function explicitly leads to divergences. After adding the counterterms (14), the long wavelength classical physics is non-divergent as the lattice spacing is taken to zero. Furthermore, these counterterms alone ensure that at high temperature, the long wavelength physics is correct and independent of the ultraviolet cutoff.

At low temperatures, however, differences between the classical and quantum theories which do not diverge with the ultraviolet cutoff become important. Such ultraviolet-finite T -dependent counterterms arise from many diagrams, not just from the two in Fig. 1. We will deal with this pragmatically, by requiring that the behavior of our partition function matches the predictions of chiral perturbation theory for $T \ll f_\pi$ and shows a critical temperature T_c in agreement with that found in lattice calculations of full QCD. In the next section, we shall use these two criteria to fix the coefficients of finite counterterms which are linear and quadratic in T .

For numerical work, it is convenient to remove the large coupling $\lambda \sim 20$ from the Langevin evolution and express all quantities in dimensionless units by scaling to new primed quantities:

$$x' = \sqrt{\lambda} v x, \quad t' = \sqrt{\lambda} v t, \quad (15)$$

$$\phi' = \frac{\phi}{v}, \quad H' = \frac{H}{\lambda v^3} \quad (16)$$

$$\eta' = \frac{\eta}{\sqrt{\lambda} v}, \quad T' = \frac{\sqrt{\lambda}}{v} T. \quad (17)$$

Using Eq. (2) gives $H' = 0.1263$. We must be careful with these rescalings since they are inconsistent with the conventional choice $\hbar = 1$. The action scales as $S \rightarrow S'/\lambda$ and so in order to leave the path integral invariant, Planck's constant \hbar must also be scaled:

$$\hbar' = \lambda \hbar. \quad (18)$$

The tadpole and sunset counterterms both scale like

$$(\Delta I)' = \frac{\Delta I}{\lambda v^2}. \quad (19)$$

Note that we do set $k_B = c = 1$ throughout.

We solve the Langevin equation on a cubic lattice using spatially periodic boundary conditions, lattice spacing a_s , and time discretization with time step a_t . We shall compare results obtained using $a_s = 0.4$ and $a_s = 1$, in dimensionless units. We always use $a_t = 0.01$. On the lattice, Eq. (4) is satisfied by choosing ξ independently at each discrete point in space and time from a random distribution with $\langle \xi \rangle = 0$ and $\langle \xi^2 \rangle = 2\eta(T)T/(a_s^3 a_t)$. We evolve the equations of motion using the fourth order symplectic algorithm, although we have also verified that using the second order algorithm suffices. We have found that these algorithms introduce much less a_t -dependence than the staggered leapfrog or stochastic Runge-Kutta algorithms.

III. ORDER PARAMETER AND CORRELATION LENGTHS

To analyze the transition we have measured the order parameter $\langle \phi \rangle$ at several temperatures, as shown in Fig. 2. We define $\langle \phi \rangle$ by

$$\langle \phi \rangle = \sqrt{\sum_{a=1}^4 \left(\frac{1}{N^3} \sum_{i,j,k=1}^N \phi_a(i,j,k) \right)^2}, \quad (20)$$

which is analogous to the magnetization in spin systems. Error bars in the figure are the standard deviation from the mean in an ensemble of a few hundred measurements along a thermalized Langevin trajectory. To determine after what time the configuration has thermalized, we monitor the system for equipartition and follow the order parameter until well after its behavior becomes non-monotonic.¹ For $H = 0$ the system suffers from critical slow-

¹To check for equipartition, we only perform the simple test of verifying that the spatial average of all four $(\partial \phi_a / \partial t)^2$ are (like the order parameter) sufficiently time-independent and are all given by T . This is equivalent to verifying that the kinetic energy of each field component is $T/2$. In effect, we are measuring the temperature of the fields, which we make sure agrees with the input value.

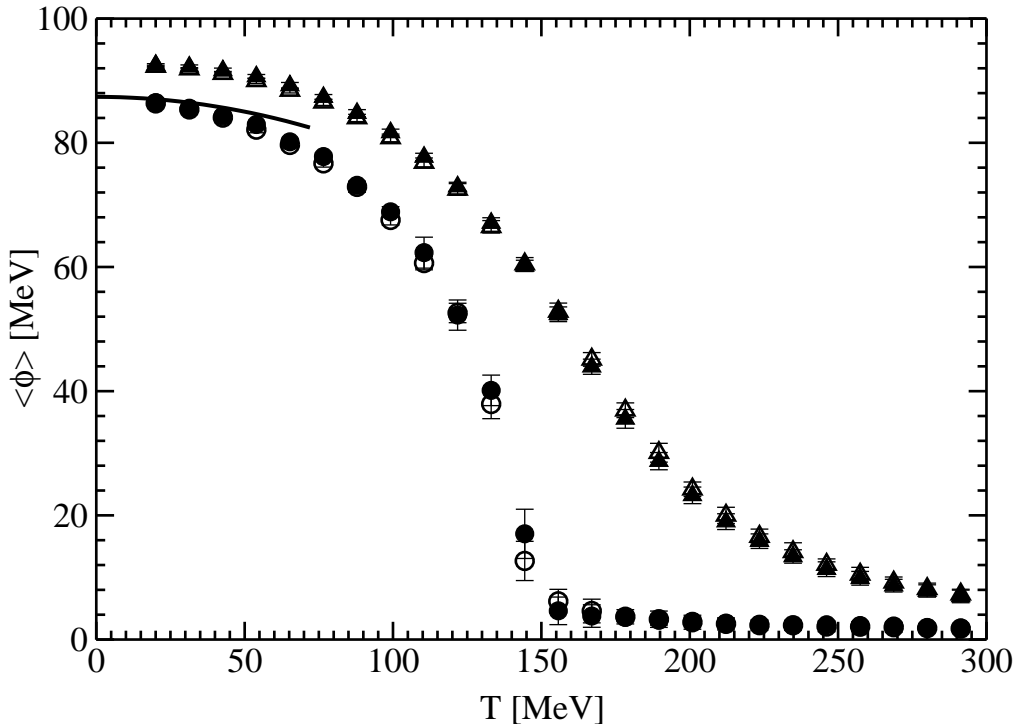


FIG. 2. The order parameter $\langle\phi\rangle$ as a function of temperature T , for $H = 0$ (circles) and H nonzero (triangles). Open and filled symbols show results obtained with $a_s = 1$ on a 26^3 lattice and $a_s = 0.4$ on a 64^3 lattice respectively, with counterterms as described in the text. The line shows the prediction from chiral perturbation theory, Eq. (21).

ing down near its critical temperature, and long Langevin trajectories are needed in order to obtain thermalization and a statistically meaningful set of measurements. For $H \neq 0$, thermalization occurs quickly at all temperatures, within a time t of order $(10 - 100)\eta^{-1}$. Langevin algorithms may yield a_t -dependent results if a_t is not chosen small enough. To exclude this possibility, we checked our order parameter measurements against those obtained from configurations thermalized using a standard Metropolis Monte Carlo algorithm.

In Fig. 2, we have required that the behavior of $\langle\phi\rangle$ agrees with the expectations from chiral perturbation theory at low temperatures [37],

$$\langle\phi\rangle = f_\pi \left(1 - \frac{T^2}{12f_\pi^2} \right), \quad T \ll f_\pi. \quad (21)$$

In particular, we have enforced the absence of linear T -dependence at small T . As anticipated in the previous section, this requires the addition of a further mass counterterm. This counterterm is not divergent in the $a_s \rightarrow 0$ limit, but it does vary with a_s . It should be thought of as coming from the order a_s^p with $p \geq 0$ contributions of infinitely many

diagrams. We find that the linear T -dependence at small T is removed upon making the replacement $-\lambda v^2 \rightarrow -\lambda v^2 + b_1 T$, with $b_1 = 0.425$ in dimensionless units. Next, we have fixed the finite counterterm proportional to T^2 . In principle, we could have done this by enforcing agreement with the coefficient of the T^2 term in (21). This is difficult in practice. Instead, we note that in the absence of any finite counterterm proportional to T^2 the second order phase transition (for $H = 0$) occurs at $T_c \simeq 130$ MeV, which is somewhat lower than that expected in QCD [28,32]. We have pushed T_c up to $T_c \simeq 150$ MeV by introducing $-\lambda v^2 \rightarrow -\lambda v^2 + b_1 T + b_2 T^2$, with $b_2 = -0.066$ in dimensionless units. These values of b_1 and b_2 were obtained with a lattice spacing $a_s = 0.4$ on a 64^3 lattice, as shown by the filled symbols in Fig. 2. To give the reader a sense of how they depend on a_s , note that on a 26^3 lattice with $a_s = 1$ (and thus the same physical volume as above) we find that with $b_2 = 0.084$ and b_1 unchanged from above, the order parameter as a function of temperature is the same as that for $a_s = 0.4$ within error bars, as shown by the open symbols in Fig. 2. We have verified that the a_s -dependence of b_2 vanishes in the weak-coupling limit and is non-divergent in the $a_s \rightarrow 0$ limit.

With $H = 0$, the order parameter shows a relatively sharp phase transition at $T = T_c \simeq 150$ MeV, which becomes sharper as the volume of the lattice is increased. At nonzero H , the explicit symmetry breaking favors the sigma direction $\langle \phi_a \rangle = \delta_{0a} f_\pi$ and the phase transition is smoothed into a crossover, which occurs over a range of temperatures somewhat above the T_c for $H = 0$. We shall see below that this crossover is centered at $T_{\text{cross}} \simeq 180$ MeV.

In addition to measuring the order parameter we have also measured the temperature dependence of the masses of the pion and sigma fields. To achieve this, we introduce a small amplitude displacement away from equilibrium in either the sigma or one of the pion field directions, and time the resulting oscillations. In practice, after first thermalizing the fields at a desired temperature as described above we add an offset in the value of the pion or sigma field to the thermalized field configuration, choosing the same offset at every point in space. We typically shift one of the pion fields by up to $0.1 f_\pi$ or shift the sigma field by up to $0.05 f_\pi$. (A larger displacement of the sigma leads to non-linear response.) We repeat this procedure for ten different realizations of a canonical thermal ensemble. The time-dependent response to the perturbation away from equilibrium is most easily measured after first averaging $\langle \pi \rangle(t)$ or $\langle \sigma \rangle(t)$ over the ensemble of runs. For small enough displacements we expect the response to be linear, and characteristic of a damped harmonic oscillator. Thus

$$\langle \phi_a \rangle = \langle \phi_a(t=0) \rangle \exp[-t/\tau] \cos(\omega t), \quad (22)$$

with $\omega = \sqrt{m^2(T) - \tau^{-2}}$ for a spatially homogeneous perturbation. Taking η small, in order to obtain large relaxation times τ , we have measured this behavior at many different temperatures. An example of the data and the fit to the form (22) is shown in Fig. 3. The results we obtain by following this procedure at many temperatures are shown in Fig. 4, together with the chiral perturbation theory prediction for the pion mass [37]

$$m_\pi^2(T) = m_\pi^2(0) \left(1 + \frac{T^2}{24 f_\pi^2} \right), \quad T \ll f_\pi. \quad (23)$$

We thus confirm that with our choice of counterterms, we are doing a good job of reproducing the predictions of chiral perturbation theory at low temperatures. We see that the sigma

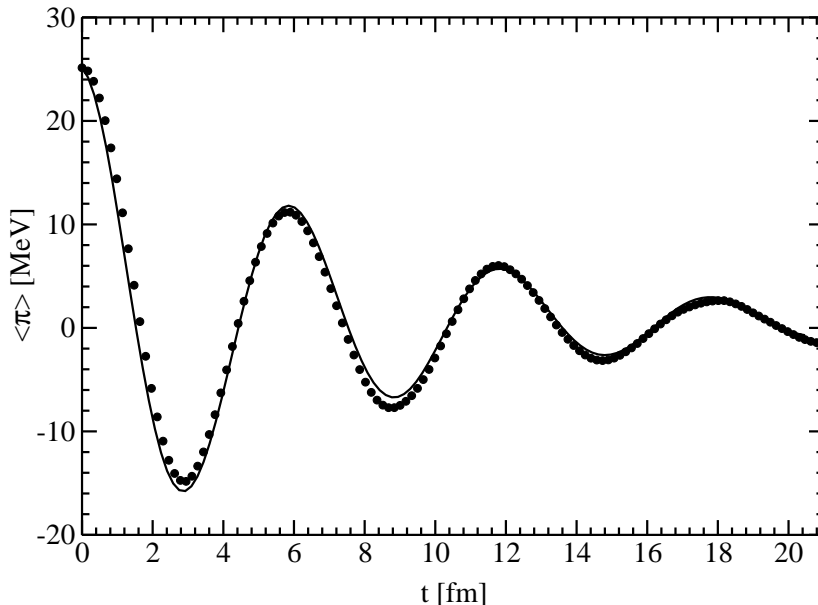


FIG. 3. An example of the fits used to determine m_π and m_σ as well as the associated decay rates. An instantaneous small perturbation away from the thermal expectation values of the fields is induced and its subsequent relaxation is fit to the form (22). In this example, we chose $\eta = 0.05$ in dimensionless units.

becomes lighter in the medium as a result of symmetry restoration at high temperatures. m_σ displays a minimum around $T_{\text{cross}} \simeq 180$ MeV, which can be taken to be the crossover temperature. At T_{cross} , $m_\pi \simeq 220$ MeV and $m_\sigma \simeq 280$ MeV. At higher temperatures, m_σ grows and m_π continues to grow monotonically. The two masses are equal within error bars for $T \gtrsim 220$ MeV.

If nature were closer to the chiral limit, m_π and m_σ would be less than T for a range of temperatures near T_{cross} , justifying our use of classical field theory for dynamics below. As it is, we shall be applying these methods somewhat beyond their regime of quantitative validity.

IV. DISORIENTED CHIRAL CONDENSATE DECAY

We have now characterized all the parameters and counterterms in the model except $\eta(T)$. η plays no role in the equilibrium physics, but it is crucial to the dynamics. In near-equilibrium dynamics, η is the parameter which controls the rate at which equilibrium is approached. To complete the characterization of our linear sigma model, we investigate the linear response timescale τ for the decay of a long wavelength pion perturbation, excited as described in the previous section. For each temperature T , we extract τ by fitting the DCC

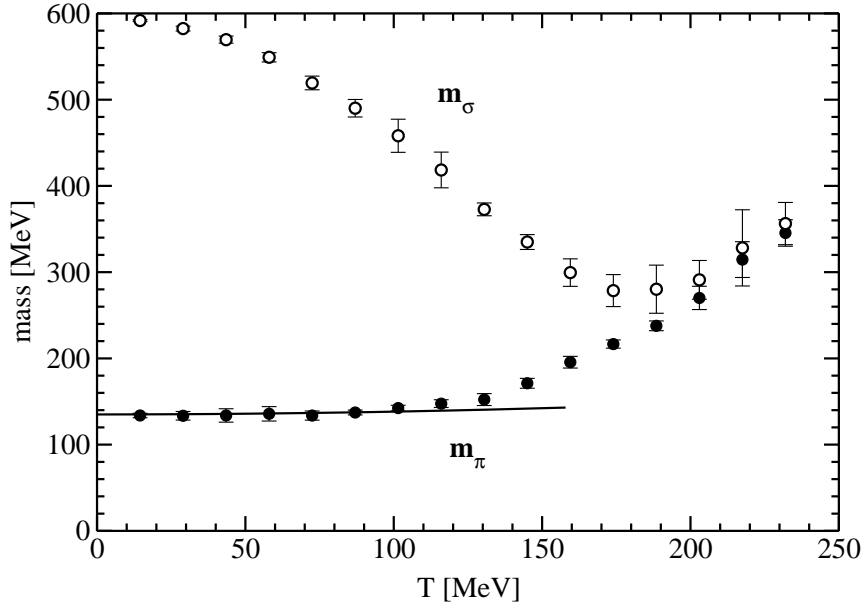


FIG. 4. The thermal masses of the σ and π fields as functions of temperature. Error bars represent statistical uncertainty in the ensemble of measurements and uncertainty in the fit, see Fig.3. The line shows the prediction from chiral perturbation theory, Eq. (23). The minimum of m_σ , which is a reasonable definition of the crossover temperature, is reached around $T_{\text{cross}} \simeq 180$ MeV. All calculations were done with $a_s = 0.4$ on a 64^3 lattice.

decay profile to the form (22). The τ so obtained depends on our choice of input η .²

The timescale $\tau(T)$ for the decay of a region of disoriented chiral condensate in contact with an equilibrated gas of hadrons has been computed previously by Steele and Koch [19]. We shall seek to choose $\eta(T)$ so that the $\tau(T)$ we then extract reproduces that calculated as in Ref. [19]. In so doing, we are normalizing the magnitude of the dissipation in the Langevin evolution to a physical observable.

The dissipation parameter $\eta(T)$ has been computed perturbatively by Rischke [20] from the imaginary part of the two-loop pion self-energy in the finite temperature quantum linear sigma model, with the result:

²Note that we only measure τ for the decay of a pion perturbation. It may also be interesting to investigate the timescale τ_σ for the relaxation of a perturbation in the sigma direction. τ and τ_σ will differ at low temperatures and become degenerate above T_{cross} . In such an investigation, one could introduce $\eta_{\sigma\sigma} \neq \eta_{\pi\pi}$, and study how τ and τ_σ depend on $\eta_{\sigma\sigma}$ and $\eta_{\pi\pi}$. Note that even though in this paper we take $\eta_{\sigma\sigma} = \eta_{\pi\pi} = \eta$, this does not mean that τ and τ_σ are equal.

$$\eta(T) = \left(\frac{4\lambda f_\pi}{N} \right)^2 \frac{m_\sigma^2}{4\pi m_\pi^3} \sqrt{1 - \frac{4m_\pi^2}{m_\sigma^2} \frac{1 - e^{-m_\pi/T}}{1 - e^{-m_\sigma^2/2m_\pi T}} \frac{1}{e^{(m_\sigma^2 - 2m_\pi^2)/2m_\pi T} - 1}}. \quad (24)$$

At $\lambda = 20$, we can only expect this calculation to be a qualitative guide.

We shall slightly extend the calculation of $\tau(T)$ performed by Steele and Koch, and so instead of simply quoting the result we first sketch their computation. We wish to analyze a large, spatially uniform, DCC in contact with a thermal gas of many other hadronic species $X = \pi, K, \dots$, which will interact with the DCC and ultimately cause it to decay. Modeling the DCC by a coherent state, and working through the LSZ formalism, Steele and Koch show that the depletion of the particles in the DCC, dN/dt , is proportional to the square of the interaction amplitudes [19]:

$$\frac{dN}{dt} = \int \frac{d^3k_1}{(2\pi)^3} \frac{d^3k_2}{(2\pi)^3} \frac{d^3k_3}{(2\pi)^3} \sum_X F_{123}^X \langle |\mathcal{T}_{\pi X}|^2 \rangle 2\pi \delta(E_0 + E_1 - E_2 - E_3) \frac{|\zeta_{k_2+k_3-k_1}|^2}{(2E_0)^2}. \quad (25)$$

For π - π scattering, the thermal weighting is given by

$$F_{123}^\pi = f_2 f_3 (1 + f_1) - f_1 (1 + f_2)(1 + f_3), \quad (26)$$

with $f_i = (\exp(E_i/T) - 1)^{-1}$ representing the Bose-Einstein momentum distribution. The DCC pion energy is $E_0 = [(k_2 + k_3 - k_1)^2 + m_\pi^2]^{1/2}$. $|\zeta|^2$ to first approximation gives the momentum-conserving delta-function leading to a formula for the half-life τ of the DCC

$$\frac{1}{N} \frac{dN}{dt} = \frac{1}{2E_0} \int \frac{d^3k_1}{(2\pi)^3} \frac{d^3k_2}{(2\pi)^3} \frac{d^3k_3}{(2\pi)^3} \sum_X F_{123}^X \langle |\mathcal{T}_{\pi X}|^2 \rangle (2\pi)^4 \delta^4(\sum k_i) \equiv -\frac{1}{\tau} \quad (27)$$

The focus of Ref. [19] was on the late time decay of a DCC, due to a heat bath with a temperature well below T_c . In this context it is reasonable to take the scattering amplitudes $\mathcal{T}_{\pi X}$ from phase-shifts of real zero-temperature data. If these are not known, then a Breit-Wigner form can be fit to the dominant resonance. To obtain the values of $\tau(T)$ shown below, $\pi\pi$ was taken from data, πK was modeled by the $K^*(892)$ resonance, $\pi\rho$ was modeled by the a_1 resonance, πN was taken from data, $\pi\bar{N}$ was taken from the same πN data, and $\pi\Delta$ ($\pi\bar{\Delta}$) was modeled by the $N^*(1675)$ resonance. Note that at $T = 170$ MeV the pions account for only about half the particles in our equilibrated resonance gas. All the other species together do play an important role. We have extended the previous analysis by including the dissipation due to πK , $\pi\Delta$ and $\pi\bar{N}$ scattering, not included in Ref. [19]. The $\tau(T)$ obtained in this way is shown in Fig. 5. The calculation is only quantitatively valid below T_c , but we have plotted the results up to higher temperatures also.

Below we shall choose $\eta(T)$ to match the decay time $\tau(T)$ of a spatially homogeneous DCC in our Langevin evolution to the values calculated by Steele and Koch. First, however, let us see what we obtain with $\eta = 0$, as in Fig. 5. That is, we first thermalize at a given temperature, add a DCC, and then set $\eta = 0$ thus removing the classical fields from further contact with any heat bath. In so doing, however, we do not remove all sources of dissipation. The long wavelength DCC still decays, by virtue of its coupling to those finite wavelength modes which we are treating classically. That is, the DCC decays via contact with an effective classical heat bath, present even for $\eta = 0$. We see that at low temperatures the resulting $\tau_{\text{cl}}(T)$ turns out to be smaller than the desired $\tau(T)$, namely that

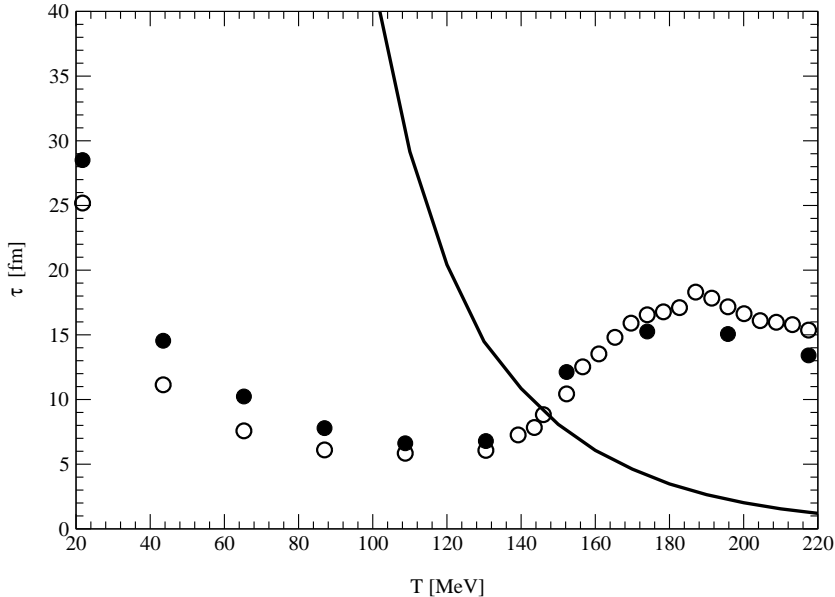


FIG. 5. The solid curve shows the decay time of a spatially homogeneous DCC via interaction with a gas of hadrons, computed following Ref. [19] as described in the text. The open (filled) circles show $\tau_{\text{cl}}(T)$, obtained from the Langevin equation with $\eta = 0$, for $a_s = 1$ ($a_s = 0.4$). The uncertainty in each point (statistical and that from the fit) is comparable to the dispersion between open and closed circles. $\tau_{\text{cl}}(T)$ reflects the dissipation of the long wavelength DCC induced by contact with thermalized classical fields at shorter wavelengths. We see that $\tau_{\text{cl}}(T) < \tau(T)$ below $T \simeq 145$ MeV.

due to contact with a gas of hadrons. The reason is that $\tau(T)$ becomes very large at low temperatures, due to the exponential suppression of the thermal occupation numbers in the (quantum) gas of hadrons. The classical thermal field theory overestimates the occupation numbers, and thus the dissipation, leading to an underestimate of τ .

Note that we have checked that our calculation of τ_{cl} is independent of the lattice spacing a_s . As shown in Fig. 5, we have compared results obtained on a 64^3 lattice with $a_s = 0.4$ to those obtained on a 26^3 lattice with $a_s = 1$. As described in the previous section, the ultraviolet-finite counterterms must be chosen differently in these two cases in order that the equilibrium behavior of the order parameter is the same in both cases. With the counterterms so adjusted, $\tau_{\text{cl}}(T)$ changes little with a_s .

The shape of $\tau_{\text{cl}}(T)$, shown in Fig. 5, is interesting and may be understood as follows. $\tau_{\text{cl}}(T)$ should grow like $1/T$ as $T \rightarrow 0$ (whereas τ grows much more rapidly in this limit). We do find that τ_{cl} rises at the lowest temperatures we have explored. The minimum of τ_{cl} coincides with the minimum value of the ratio $m_\pi(T)/T$, which occurs at $T \simeq 120\text{--}130$ MeV. This means that the classical thermal pions are most numerous in this temperature regime, making it plausible that the classical dissipation is largest and τ_{cl} is smallest.

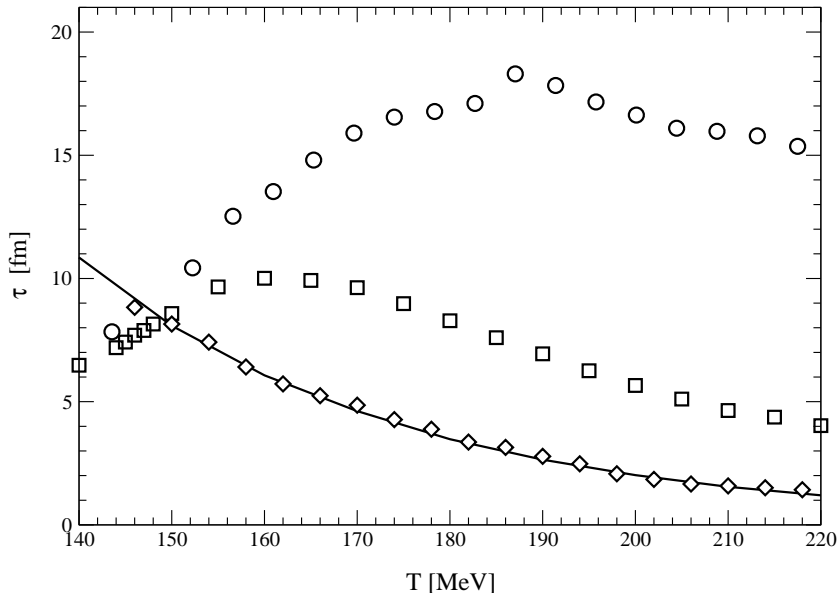


FIG. 6. Circles show the DCC decay time $\tau_{\text{cl}}(T)$ for the classical σ -model at $\eta = 0$. Squares show $\tau(T)$ obtained from the Langevin equation with $\eta(T)$ taken from Rischke's perturbative calculation. Diamonds show $\tau(T)$ obtained from the Langevin equation with $\eta(T)$ chosen so as to reproduce $\tau(T)$ from the calculation of Steele and Koch, shown as the solid line. Errors are similar to those discussed for Fig. 5.

We now see the challenge posed by our use of a classical theory, with its intrinsic decay time $\tau_{\text{cl}}(T)$. By turning on a nonzero η , we can only add dissipation. This means that we can only reduce τ , relative to $\tau_{\text{cl}}(T)$. At temperatures where $\tau_{\text{cl}}(T) < \tau(T)$, therefore, there is no way to use our Langevin equation to reproduce the correct dynamics of the decay of a DCC. Thus, we find that our model can only be used to describe the long wavelength dynamics in the presence of a heat bath with $T \gtrsim 145$ MeV, corresponding to about 80% of the crossover temperature T_{cross} . $T \sim 145$ MeV is large enough that the assumptions in the calculation of τ as in Ref. [19] may be starting to break down, which means that our estimate of the limit of validity of our analysis may have a little play in it. However, the fundamental fact that τ should rise rapidly with decreasing temperature while τ_{cl} does not is incontrovertible.

Above $T \simeq 145$ MeV, we can proceed as planned. We can choose an $\eta(T)$ in such a way as to reproduce the predictions of Steele and Koch, as demonstrated in Fig. 6. The required $\eta(T)$ is plotted in Fig. 7, where it is also compared to the $\eta(T)$ of Eq. (24), calculated perturbatively by Rischke [20]. We see (from both Figs. 6 and 7) that introducing the perturbatively calculated $\eta(T)$ into the Langevin equation is not sufficient to obtain a DCC decay timescale $\tau(T)$ in agreement with that induced via contact with a thermal hadron

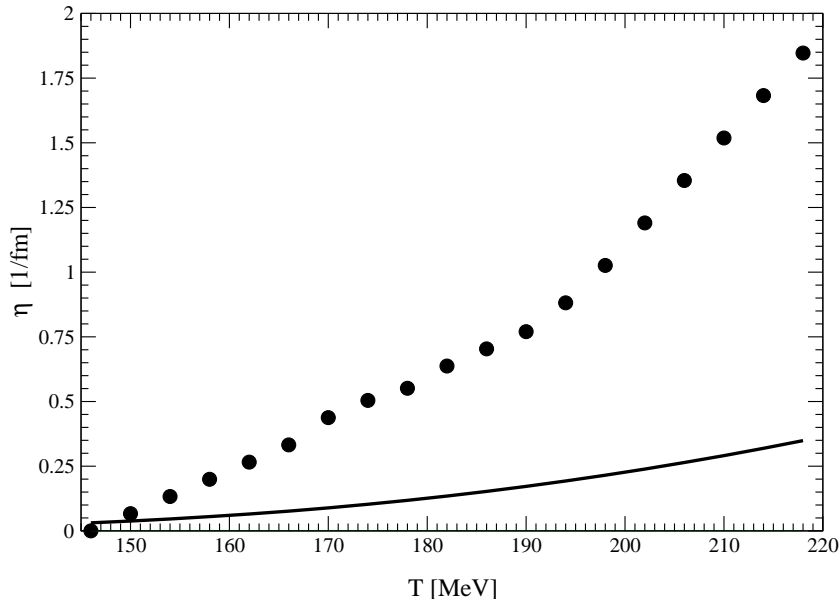


FIG. 7. $\eta(T)$ from Rischke's perturbative calculation (solid line) and $\eta(T)$ chosen so that the Langevin equation reproduces $\tau(T)$ computed by Steele and Koch (circles).

gas.³ Both the calculations of Rischke and of Steele and Koch are only of quantitative validity below T_c , as they use zero temperature masses and interactions. Nevertheless, the discrepancy between the $\eta(T)$'s in the vicinity of T_c is sufficiently large that we take this to mean that, for $\lambda = 20$, the perturbative calculation underpredicts η .

V. DISCUSSION

We have shown how to use a stochastic classical linear sigma model to obtain a reasonable description of the equilibrium thermodynamics and the long-wavelength near-equilibrium dynamics of QCD at temperatures of order that of its phase transition. The use of any classical statistical field theory around the chiral transition cannot be quantitatively justified, because there are no excitations with masses which are very small compared to the temperature. Nevertheless, we have determined the choice of divergent counterterms needed

³It is not clear whether we should have expected the use of η from (24) to yield too rapid or too slow dissipation. On the one hand, we may have expected that use of the perturbative $\eta(T)$ in the Langevin equation would yield excess dissipation, as there is always classical dissipation in addition. On the other hand, we may have expected that it would introduce insufficient dissipation, as its calculation neglects the effects of all hadrons in the heat bath except the pions and sigma.

to remove the ultraviolet divergences from the classical linear sigma model, making the long distance physics described therein independent of the lattice spacing. We have then been able to find the finite counterterms needed in order for the equilibrium temperature dependence of the order parameter in the linear sigma model to be as in QCD at low temperatures, as calculated in chiral perturbation theory, and for T_c to be as in QCD, as calculated in lattice gauge theory. The temperature dependence of the pion and sigma masses then come out nicely in accord with expectations. We have then fixed $\eta(T)$ such that the timescale for the dissipation of a DCC in our Langevin model agrees with that calculated previously. The main constraint on our model is that it cannot be used at low temperatures, where the classical dissipation is too great even when η is set to zero. We find that this limits its use to temperatures above about 80% that of the crossover transition itself. Above this temperature, we show how to choose $\eta(T)$ in such a way that the long wavelength dynamics of the pions and sigma should be reproduced reasonably well in our model, at least as long as the system is not too far out of thermal equilibrium.

In this work, we have used the dynamics of an idealized DCC as a device with which to normalize our model. In subsequent work, we shall use the now normalized model to investigate the dynamical setting where the system expands and cools through its chiral crossover transition. We hope to determine with some confidence how fast the expansion and cooling must be in order for the dynamics to be driven significantly from equilibrium. We will then follow the nonequilibrium long wavelength evolution for as long as occupation numbers remain reasonably high. Unlike in the idealized setting utilized for convenience in this paper and in the analytic computations of $\eta(T)$, the long wavelength modes will certainly not describe a spatially uniform condensate.

ACKNOWLEDGEMENTS

KR is grateful to D. Rischke for long discussions several years ago which started DR down the path toward Ref. [20] and started KR down the path toward the present paper. We also acknowledge conversations with A. K. Chaudhuri. Numerical work was performed in part at the T-Division/CNLS Avalon cluster at Los Alamos National Laboratory. This work is supported in part by the Department of Energy under cooperative research agreement #DF-FC02-94ER40818. The work of KR was supported in part by a DOE OJI Award and by the A. P. Sloan Foundation.

REFERENCES

- [1] R. Baier, A. H. Mueller, D. Schiff, and D. T. Son, Phys. Lett. B **502**, 51 (2001) [hep-ph/0009237].
- [2] K. H. Ackermann *et al.* [STAR Collaboration], Phys. Rev. Lett. **86**, 402 (2001) [nucl-ex/0009011].
- [3] A. Barducci, R. Casalbuoni, S. DeCurtis, R. Gatto, G. Pettini, Phys. Lett. B **231**, 463 (1989); S.P. Klevansky, Rev. Mod. Phys. **64**, 649 (1992); A. Barducci, R. Casalbuoni, G. Pettini and R. Gatto, Phys. Rev. D **49**, 426 (1994); M. Stephanov, Phys. Rev. Lett. **76**, 4472 (1996); Nucl. Phys. Proc. Suppl. **53**, 469 (1997); J. Berges and K. Rajagopal, Nucl. Phys. B **538**, 215 (1999) [hep-ph/9804233]; M. A. Halasz, A. D. Jackson, R. E. Shrock, M. A. Stephanov and J. J. Verbaarschot, Phys. Rev. D **58**, 096007 (1998) [hep-ph/9804290].
- [4] M. Stephanov, K. Rajagopal and E. Shuryak, Phys. Rev. Lett. **81**, 4816 (1998) [hep-ph/9806219].
- [5] M. Stephanov, K. Rajagopal and E. Shuryak, Phys. Rev. D **60**, 114028 (1999) [hep-ph/9903292].
- [6] For a review see K. Rajagopal, Acta Phys. Polon. B **31**, 3021 (2000) [hep-ph/0009058].
- [7] K. Rajagopal, Nucl. Phys. A **680**, 211 (2000) [hep-ph/0005101].
- [8] See, for example, H. Heiselberg and A. D. Jackson, nucl-th/9809013; I. N. Mishustin, Phys. Rev. Lett. **82**, 4779 (1999) [hep-ph/9811307].
- [9] B. Berdnikov and K. Rajagopal, Phys. Rev. D **61**, 105017 (2000) [hep-ph/9912274].
- [10] K. Rajagopal and F. Wilczek, Nucl. Phys. B **404**, 577 (1993) [hep-ph/9303281].
- [11] A. A. Anselm, Phys. Lett. B **217**, 169 (1988); A. A. Anselm and M. G. Ryskin, Phys. Lett. B **266**, 482 (1991).
- [12] J. Blaizot and A. Krzywicki, Phys. Rev. D **46**, 246 (1992).
- [13] J. D. Bjorken, Int. J. Mod. Phys. **A7**, 246 (1992); *ibid.*, 4189; J. D. Bjorken, Acta Phys. Polon. B **23**, 637 (1992); K. L. Kowalski and C. C. Taylor, hep-ph/9211282; J. D. Bjorken, K. L. Kowalski and C. C. Taylor, hep-ph/9309235.
- [14] K. Rajagopal and F. Wilczek, Nucl. Phys. B **399**, 395 (1993) [hep-ph/9210253].
- [15] M. M. Aggarwal *et al.* [WA98 Collaboration], Phys. Lett. B **420**, 169 (1998) [hep-ex/9710015]. M. M. Aggarwal *et al.* [WA98 Collaboration], Phys. Rev. C **64**, 011901 (2000) [nucl-ex/0012004].
- [16] C. Greiner, C. Gong and B. Muller, Phys. Lett. B **316**, 226 (1993) [hep-ph/9307336]. Z. Huang, M. Suzuki and X. Wang, Phys. Rev. D **50**, 2277 (1994) [hep-ph/9403300]; S. Gavin, Nucl. Phys. A **590**, 163 (1995); hep-ph/9407368; Z. Huang, I. Sarcevic, R. Thews and X. Wang, Phys. Rev. D **54**, 750 (1996) [hep-ph/9511387]; Z. Huang and X. Wang, Phys. Lett. B **383**, 457 (1996) [hep-ph/9604300]; D. Boyanovsky, H. J. de Vega, R. Holman and S. Prem Kumar, Phys. Rev. D **56**, 5233 (1997) [hep-ph/9701360]; Phys. Rev. D **56**, 3929 (1997) [hep-ph/9703422]; Y. Kluger, V. Koch, J. Randrup and X. Wang, Phys. Rev. C **57**, 280 (1998) [nucl-th/9704018]; H. Hiro-Oka and H. Minakata, Phys. Lett. B **425**, 129 (1998) [Erratum-*ibid.* B **434**, 461 (1998)] [hep-ph/9712476]; T. C. Petersen and J. Randrup, Phys. Rev. C **61**, 024906 (2000) [nucl-th/9907051]; C. Chow and T. D. Cohen, Phys. Rev. C **60**, 054902 (1999) [nucl-th/9908013]; J. I. Kapusta and S. M. Wong, Phys. Rev. Lett. **86**, 4251 (2001) [nucl-th/0012006].
- [17] F. Cooper, S. Habib, Y. Kluger, E. Mottola, J. P. Paz and P. R. Anderson, Phys. Rev.

- D **50**, 2848 (1994) [hep-ph/9405352]; D. Boyanovsky, H. J. de Vega, and R. Holman, Phys. Rev. D **51**, 734 (1995) [hep-ph/9401308]; F. Cooper, Y. Kluger, E. Mottola, and J. Paz, Phys. Rev. D **51**, 2377 (1995) [hep-ph/9401308]; M. A. Lampert, J. F. Dawson and F. Cooper, Phys. Rev. D **54**, 2213 (1996) [hep-th/9603068]; F. Cooper, Y. Kluger, E. Mottola, Phys. Rev. C **54**, 3298 (1996) [hep-ph/9604284]; D. Boyanovsky, F. Cooper, H. J. de Vega and P. Sodano, Phys. Rev. D **58**, 025007 (1998) [hep-ph/9802277].
- [18] M. Asakawa, Z. Huang and X. Wang, Phys. Rev. Lett. **74**, 3126 (1995) [hep-ph/9408299].
- [19] J.V. Steele, and V. Koch, Phys. Rev. Lett. **81**, 4096 (1998) [nucl-th/9806055].
- [20] D. H. Rischke, Phys. Rev. C **58**, 2331 (1998) [nucl-th/9806045].
- [21] C. Greiner and B. Muller, Phys. Rev. D **55**, 1026 (1997) [hep-th/9605048].
- [22] Z. Xu and C. Greiner, Phys. Rev. D **62** 036012 (2000) [hep-ph/9910562].
- [23] T. S. Biro and C. Greiner, Phys. Rev. Lett. **79**, 3138 (1997) [hep-ph/9704250].
- [24] A. K. Chaudhuri, Phys. Rev. D **59**, 117503 (1999) [nucl-th/9809018]; J. Phys. G **27** 175 (2001) [hep-ph/9908376]; hep-ph/0007332; hep-ph/0011003.
- [25] A. K. Chaudhuri, hep-ph/0105013.
- [26] J. Randrup, Phys. Rev. Lett. **77**, 1226 (1996) [hep-ph/9605223]; Nucl. Phys. A **616**, 531 (1997) [hep-ph/9612453]; J. Randrup, Phys. Rev. C **62**, 064905 (2000) [nucl-th/0010104].
- [27] R. Pisarski and F. Wilczek, Phys. Rev. D **29**, 338 (1984); F. Wilczek, Int. J. Mod. Phys. A **7**, 3911 (1992).
- [28] S. Gottlieb et al., Phys. Rev. D **55**, 6852 (1997) [hep-lat/9612020].
- [29] R. D. Pisarski, Phys. Rev. D **62**, 111501 (2000) [hep-ph/0006205]; A. Dumitru and R. D. Pisarski, Phys. Lett. B **504**, 282 (2001) [hep-ph/0010083].
- [30] S. Datta and S. Gupta, Nucl. Phys. B **534**, 392 (1998) [hep-lat/9806034].
- [31] R. V. Gavai and S. Gupta, Phys. Rev. Lett. **85**, 2068 (2000) [hep-lat/0004011].
- [32] For reviews, see F. Karsch, Nucl. Phys. Proc. Suppl. **83**, 14 (2000) [hep-lat/9909006]; E. Laermann, Nucl. Phys. Proc. Suppl. **63**, 114 (1998); and A. Ukawa, Nucl. Phys. Proc. Suppl. **53**, 106 (1997).
- [33] L. M. A. Bettencourt, Phys. Rev. D **63**, 045020 (2001) [hep-ph/0005264].
- [34] P.C. Hohenberg and B.I. Halperin, Rev. Mod. Phys. **49**, 435 (1977).
- [35] G. Parisi, Statistical Field Theory (Addison-Wesley, New York, 1988).
- [36] K. Farakos, K. Kajantie, K. Rummukainen, M. Shaposhnikov, Nucl. Phys. B **425**, 67 (1994) [hep-ph/9404201].
- [37] P. Gerber and H. Leutwyler, Nucl. Phys. B **321**, 387 (1989); R. D. Pisarski and M. Tytgat, Phys. Rev. D **54**, 2989 (1996) [hep-ph/9604404].